This article has been accepted for publication in a future issue of this journal, but has not been fully edited. Content may change prior to final publication. Citation information: DOI 10.1109/JSEN.2018.2854271, IEEE Sensors Journal

A Capacitive Strip Sensor for Detecting Partial Discharge in 110 kV XLPE Cable Joints

Jun Jiang, Zhendong Ge, Mingxin Zhao, Miao Yu, Xuewei Chen, Min Chen and Jiansheng Li

Abstract— **The joints of Cross Linked Poly Ethylene (XLPE) power cables often suffer the frequent faults and latent defects, which can be detected effectively by partial discharge (PD). In this study, a novel capacitive strip sensor for PD measurement is proposed and testified under the context of prefabricated 110kV XLPE cable joints. Firstly, a simulation model based on Finite Integration Technique (FIT) is established. Then the transmission mode and the frequency spectrum of the electromagnetic wave related to the PD signal is investigated. Furthermore, the energy distribution of PD signal among the cable joint is analyzed to identify the optimal position of installation. Finally, a real capacitive strip PD detection sensor is deployed on a 110kV XLPE cable system and comparative tests with a standard sensor are conducted. Consistent experimental results have been observed and a sensitivity better than 5 pC has been achieved on the proposed capacitive strip sensor, which clearly shows its potential on online PD monitoring for high voltage power cable joints.**

Index Terms **— power cables, monolithic insulated joint, partial discharge, sensor, Finite integration technique**

I. Introduction

Cross Linked Poly Ethylene (XLPE), has been widely used as the insulation of high voltage cables due to its excellent electrical, thermal and mechanical characteristics[1, 2]. The XLPE cables are especially welcomed at various voltage levels of underground grid in urban areas [3]. For XLPE cables, their joints are often the weakest insulation parts due to dielectric insulation discontinuity and the unavoidable construction related flaws [4, 5]. Insulation problems easily lead to partial discharge (PD) phenomenon, which is a localized dielectric breakdown of a small portion of the solid or gas electrical insulation. Over time, PD would lead to electrical treeing and impair the insulation strength of the cable (or joint). This could considerably reduce the life span of these high voltage power XLPE cables [6]. Thus, it is of great importance to detect and monitor PD activities to support asset management decisions, especially with the trend of Condition Based Maintenance (CBM) [7].

Up to now, there are mainly electrical and non-electrical categories for online PD detection techniques of XLPE cables. Non-electrical techniques include acoustic emission (AE) method [8, 9] and electro-optic (EO) method [10-12]. These techniques have the advantages of easy installation, non-destructive testing (NDT), and anti-electromagnetics, et al. However, acoustic sensors are often suffered from the background acoustic noises while electro-optic systems are usually relatively expensive to be implemented. Therefore, electrical techniques are the mainstream approaches in this particular field. Electrical technique based PD detection equipment include high frequency current transformers (HFCT), directional couplers (DCS), foil electrodes, and Ultra-High Frequency (UHF) sensors, et al. [10]

In most situations, the sensors installed outside the power cable joints are researched and developed owing to their easy installation. By detecting the high frequency current pulses generated by PD, HFCT sensors are most widely applied for PD detection in XLPE cables. The frequency band of HFCT sensors is usually from hundreds of kHz to dozens of MHz, which has been proven to be capable of capturing PD signals [13-15]. Split-core HFCT sensors are convenient to install and meet the PD measuring standard IEC 60270 [16] well. Nevertheless, special issues such as noise reduction and dynamic range have to be taken into consideration due to the complex electromagnetic effect and interferences [17, 18]. Other PD detection equipment like the DCS [19, 20] and foil electrodes [21], which are placed outside the power joints are also prone to these issues. In addition, the semiconducting layers of XLPE cables would absorb the energy of the partial discharge signal, and lead to significant attenuation and distortion effects on the high frequency components of PD signal. Ultra-High Frequency (UHF) sensors are relatively robust to external noises and disturbances [22], and perform well in transformers and gas insulated switchgears (GIS). UHF techniques with the general frequency band of 300 MHz -3000 MHz, are able to detect PD activity through electromagnetic waves. However, the metal shielding layer in XLPE cables blocks the electromagnetic wave [13, 23, 24], making the UHF sensors unsuitable to be used in power cables.

Generally speaking, the external sensors are vulnerable to environmental interference and often poor in detection

Manuscript received 23/01, 2018. This work was supported in part by the Fundamental Research Funds for the Central Universities (NO. XCA17003-04, NS2018027), the State Key Laboratory of Alternate Electrical Power System with Renewable Energy Sources (Grant No. LAPS17012), Natural Science Foundation of Jiangsu Province (BK20170786) and State Grid Zhejiang Electric Power Co. Ltd. (5211DS17001C).

Jun Jiang and Mingxin Zhao are with the Center for more-electric-aircraft power system, Nanjing University of Aeronautics and Astronautics, Nanjing 210016, China (corresponding e-mail: jiangjun0628@163.com); Zhendong Ge is with Beijing Electric Power Company, State Grid Corporation of China, Qianmenxi Street #41, Beijing 100031, China; Miao Yu and Jiansheng Li are with State Grid Jiangsu Electric Power Co. Ltd. Research Institute, Nanjing 211103, China; Xuewei Chen is with the State Grid Jiangsu Electric Power Co. Ltd. Nanjing Power Supply Company, Nanjing 210019, China; Min Chen is with State Grid Zhejiang Electric Power Co. Ltd. Research Institute, Hangzhou 310014, China.

sensitivity, which makes them unsuitable for online monitoring for a long time. Therefore, an inside-the-joint solution based on the electromagnetic (EM) conversion principle, with inductive strip sensors and EM coupling sensors were investigated to PD detection [25-27]. Unfortunately, the inductive strip sensors can be only used for the twisted screen wire cables with low sensitivity due to the small mutual inductance. Instead of the inductive strip sensors, a capacitive sensor made up of a thin copper tape, is much easier and cheaper to produce and install.

In this study, a capacitive strip sensor detecting partial discharge is proposed inside the structure of 110 kV monolithic insulated joints. A space capacitor is constituted by the cable core conductor and an additional copper strip, which locates at the break position of the outside semiconducting layer of the cable. To evaluate the optimal installation of the strip sensor and propagation frequency of partial discharge, an accurate model of cable joint based on Finite integration technique is established and the optimal measurement frequency band is obtained. Then a 110kV cable partial discharge test platform was set up. Comparative experiments are conducted to testify the effectiveness of the proposed capacitive strip sensor.

II. Simulation Analysis

A. Modelling of cable joints

XLPE cables at the voltage level of 110kV and above are usually single-core structure. Because of the induced electromotive force (EMF) on the metal shield of the cable, reliable grounding of the high voltage XLPE cables is of great importance. Especially, when the cable is longer than 1000 meters, a cross-bonding cable system is preferred and recommended. The cross-bonding is to divide the cable into different sections of equal length. And monolithic insulated joints are installed between every two sections: Phase A to Phase B, Phase B to Phase C, Phase C to Phase A, as illustrated in Fig. 1. This method can reduce the induced electromotive voltage and circulating current on the metal sheath and improve the transmission capacity of power cables.

According to the manufacturing process of the monolithic insulated joint, the outer surface of the main silicone rubber insulation is covered by a semi-conductive coating as an insulating shield. The insulating shield is wrapped around by the grounding copper wire mesh. Near the end of the insulated joint there is a section without insulation shielding and insulation part of the grounding copper mesh. This section is to disconnect the electrical connection between the metal shielding layer on both sides of the cable and the insulation shield (that is, the outer semi-conductive layer). The structure of the described monolithic insulated joints is shown in Fig.1.

The internal structure of the cable intermediate connector is complex and there are many dielectric interfaces. Especially, the stress cone, used to uniformize the interfacial tangential electric field, is made up of a nonlinear lossy semicon material. Therefore, the propagation of PD magnetic waves in the connector is greatly attenuated and distorted.

To provide the basis for the reasonable design and installation of the detection sensor, it is essential to analyze the propagation law of the partial discharge electromagnetic wave in the intermediate joint.

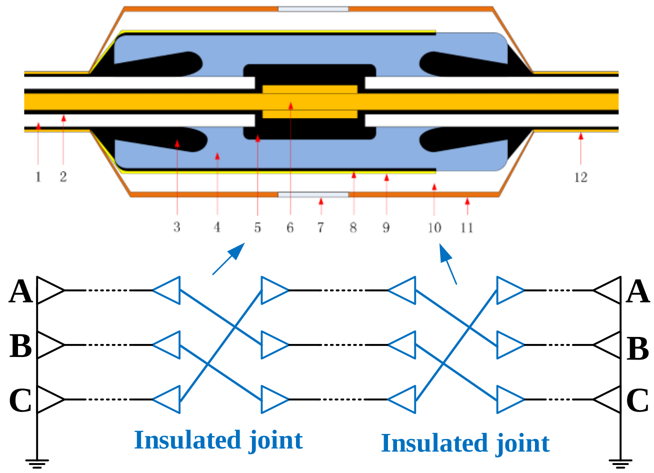

1- XLPE insulation; 2- inner semi-conductive layer; 3- stress cone; 4- silicone rubber insulation; 5- inner field control layer; 6- conductor and connector; 7- epoxy resin; 8- outer semi-conductive layer; 9- copper wire sleeve; 10- polyurethane sealant layer; 11- copper protection tube; 12- jacket.

Figure 1 Schematic diagram of a cross-bonded three-phase cable system and a monolithic insulated joint

Based on the real 110kV cable intermediate joint structure, HL-YJJJ / JTI, a simulation model of cable insulation type intermediate joint was established. Since its complex structure, the meshing needs to be particularly intensive during the simulation, and the cable intermediate joint structure has to be reasonably simplified, as shown in Fig.2. Connector and conductor were combined as one. Additionally, the grounding copper wire sleeve is simplified as copper skin, owing to the actual diameter of the copper mesh was only about 0.1 mm. Finite Integration Technique (FIT) is selected due to its high flexibility in geometric modeling and boundary handling as well as incorporation of arbitrary material distributions and material properties such as anisotropy, non-linearity and dispersion.

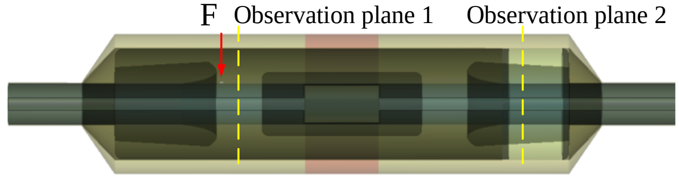

Figure 2 Structure model of monolithic insulated joint

Table 1 gives the parameters of materials in the 110 kV cross-bonded cable joint and Fig.3 shows the frequency dependent permittivity/conductivity of the semicon material in the inner/outer semiconducting layers and stress cones. Then complex permittivity of semicon material could be obtained with the fitting curve of the data, according to Equation 1.

$$\varepsilon = \varepsilon_0(\varepsilon' - j\varepsilon'') = \varepsilon_0(\varepsilon' - j\frac{\sigma}{\omega}) \tag{1}$$

Table 1 Material specifications of the cross-bonded cable joint

Material	Relative permittivity	Conductivity (S/m)
XLPE	2.5	0
Silicon rubber	3.2	0
Epoxy resin	5.0	0.0055

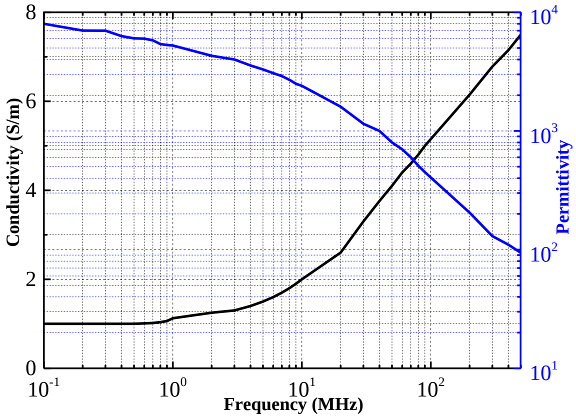

Figure 3 Frequency dependent permittivity of the semicon material [28]

B. Excitation and boundary setting

Point F in Fig.2, is the needle defect location in the silicone rubber and XLPE insulation at the interface, is added in the cable joint model to represent as an excitation source of partial discharge. The negative mathematical model using current source of needle defect could be calculated from Ref. [29], as shown in Fig.4.

Since the excitation source spectrum is mainly distributed within 600 MHz, the maximum frequency is set to 1 GHz in this simulation. It is not accurate to set the maximum frequency close to that of PD source because the signal-to-noise ratio (SNR) is quite low at the sideband.

In the boundary condition setting, an open boundary with perfectly matched layers (PML) is used to simulate an infinite space, through which the electromagnetic waves could pass freely without reflection.

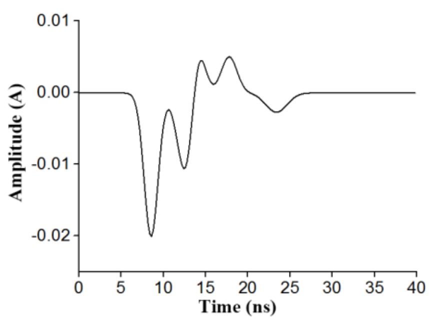

Figure 4 Waveform shapes of partial discharge pulse generated by negative needle defect

C. PD propagation mode

Signals propagate within waveguides in various modes: TE (Transverse Electric), TM (Transverse Magnetic), TEM (Transverse Electric and Magnetic). Each mode has different orders. The text about the different types of indicating TE and TM waveguide modes is written as integers after them: $TE_{m,n}$. The structure of power cable joint can be seen as the coaxial waveguide. The lowest cut-off frequency f_c of waveguide TE_{11} is easy to be calculated from:

$$f_c = \frac{1}{\pi\sqrt{\mu\varepsilon}(a+b)} \tag{2}$$

With regard to 110kV power cables, the conductor section is 50 mm^2. The inner conductor radius a equals 9 mm, and the outer conductor radius b is 82 mm. The intermediate joint media can be simplified as a unified silicone rubber leaving out of the XLPE and semiconducting layer, and the cut-off frequency can be calculated as 586 MHz. Considering that the PD signal spectrum distribution needle defect is within 600 MHz, and the higher the frequency, the more serious the attenuation during the propagation.

In order to analyze the propagation mode of the electromagnetic wave inside the cable joint, two observation planes were selected as shown in Fig.2 and Fig.5. There are 4 detection points A1, B1, C1 and D1 on the observation plane 1 (shown in Fig. 5a), which is 20 mm away from the excitation source F. A1 is located right above PD source with 0° angle, and the remaining points are arranged inside the insulation shield with the intervals of 90 ° clockwise. Similar setting of plane 2 can be seen in Fig.5b.

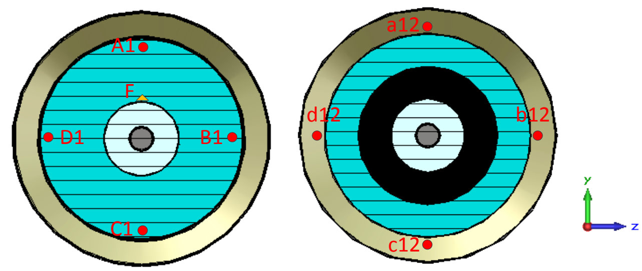

a) Observation plane 1 b) Observation plane 2

Figure 5 Layout of detection points in observation planes

The electric field distributions of A1 and B1 are shown in Fig. 6 and Fig. 7 respectively. It can be seen that the magnitudes of Ey at point A1 and Ez at point B1 are higher than the other two directional components at least one order in magnitude, which indicates the radial field strength component is the largest. The electric field in the non-radial direction is weak mainly due to the complex structure of the power cable joint has various internal media and the refraction at the interface of all layers, rather than the ideal coaxial waveguide structure. Therefore, the electromagnetic field inside the cable joint propagates in a quasi-TEM mode.

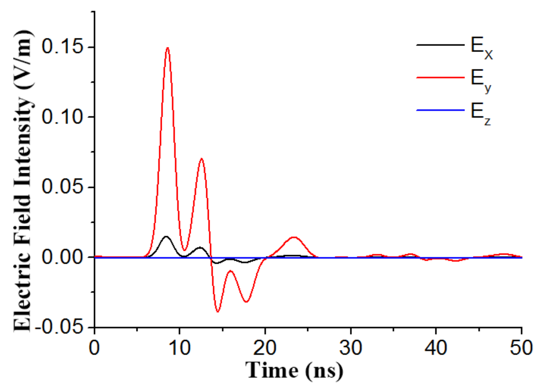

Figure 6 Electric field strength component of A1 position

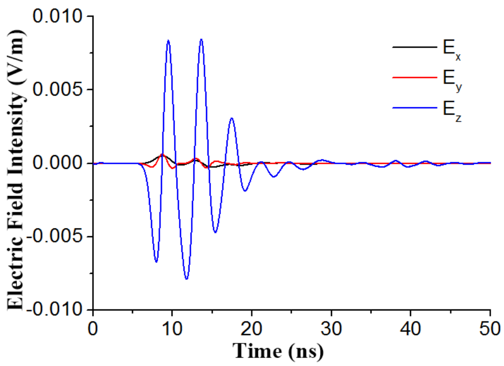

Figure 7 Electric field strength component of B1 position

D. PD attenuation characteristics

The strip sensor is designed to be installed inside the protection tube, and partial discharge signal (electromagnetic wave) attenuated in the cable joint. Points A1 to A13 were set on the same horizontal line inside the insulating shield, separated by 40 mm at each point with the PD source at the angle of 0°, as shown in Fig. 5. Similarly, a series of points a1 to a13 were set between the grounded copper mesh and the protection tube; points E1 to E5 were located outside of the protection tube. All these points were used to analyze the attenuation characteristics of the electromagnetic field propagating in the power cable joint.

The amplitude of the electric field at the observation points changes with time and generally attenuates at around 50 ns. The energy of the electromagnetic wave is proportional to the square of the electric field over time in 50 ns, as shown in Equation (3). Therefore, it's easy to compare the electromagnetic wave energy at each detection point within 50 ns. The partial discharge amplitude and energy could be normalized by the Equation (4).

$$W \propto \int_0^{50} \mathrm{E(t)}^2 dt \tag{3}$$

$$W_i^* = 10\log\frac{W_i}{W_{\max}} \tag{4}$$

It can be seen that the energy of the electromagnetic wave inside the joint decays rapidly away from the PD source, but slightly increases in the range of -80 ~ 80mm, as show in Fig.8. The reason is that the small space conductive silicone and metal shield in this area resulting in enhanced reflection of electromagnetic waves. Additionally, due to the existence of stress cone in the range of 200 ~ 240 mm, the energy increases in this range as well. The electromagnetic waves transmitted from the left are repeatedly reflected between the stress cone and the metal shield so that the energy in this area is enhanced.

The signal attenuation in the area between the connector and the copper protection tube is shown in Fig. 9. The energy is more concentrated in the right part of the protection tube, since the copper tube is equivalent to a resonant cavity, where the signal radiated from the insulation section is subjected to multiple refractions within the area. On the contrary, lower energy intensity distributed in the middle part of -80 ~ 80mm, because the energy radiated to the outside and left part of copper protection tube. Inside the left copper tube there are also refractions. In detection points E1 ~ E5 outside of the copper tube, the energy intensity decreased to 1/10 ~ 1/100 of inner protection tube.

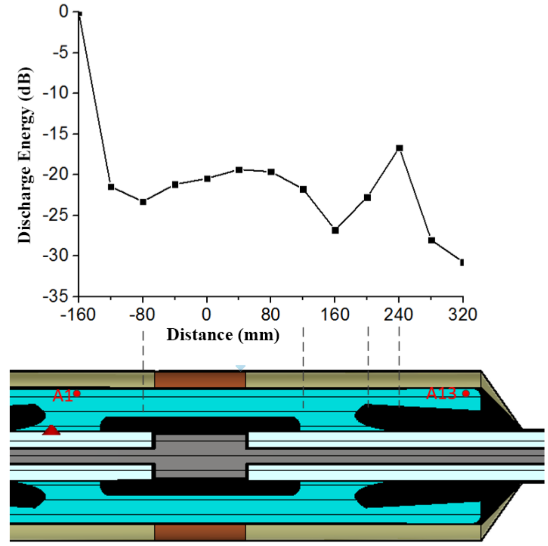

Figure 8 Energy distribution curve of A1~A13 positions

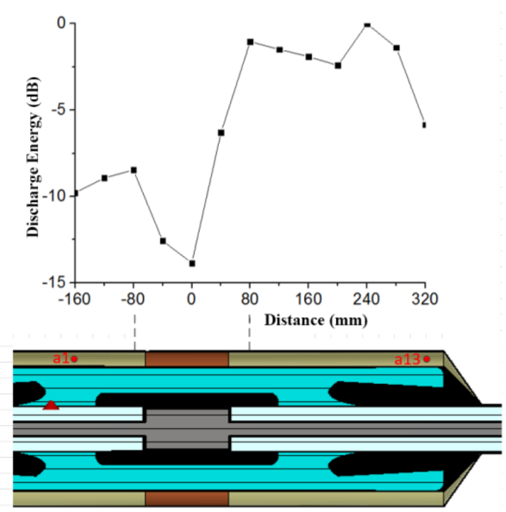

Figure 9 Energy distribution curve of a1~a13 positions (copper protection tube)

Therefore, the best installation position of the detection sensor locates in between the insulation part and the protection tube, in particular at the position around the stress cone.

E. Frequency spectrum analysis

The optimal dimension of the strip sensor is set as, the longitude length: 50 mm, the diameter: 82 mm and the thickness: 0.5 mm. To analyze the frequency spectrum of the PD detection, position a13 is selected. The frequency band of the signal mainly concentrates between 50 MHz and 300 MHz, with two resonance peaks of 75 MHz and 245 MHz, as shown in Fig.10.

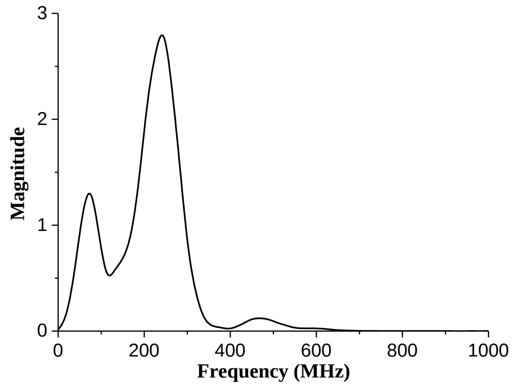

Figure 10 Frequency spectrum of a13 position

III. Partial Discharge Detection of Monolithic Insulated Joint

A. PD measurement system based on the strip sensor

Since the semiconducting layer has a certain attenuation and distortion effect on the partial discharge signal propagation, it will have a negative effect on the partial discharge measurement. Therefore, the design of the PD sensor should avoid the influence of the semi-conductive layer in order to obtain higher measurement sensitivity. As aforementioned, there is a zone of interrupted outer semi-conductive layer near the ends of the insulation connector. In our design, a metal strip was wrapped around the insulating surface in this area as a detection sensor. The schematic diagram of radial section is shown in Fig.11 (a). A space capacitor was formed by the strip sensor and the cable core to couple the PD signal inside the insulation layer. The strip sensor was grounded via a 50Ω non-inductive resistor. It could receive the partial discharge pulse voltage signal coupled from both ends of the resistor. The detected signal is then transferred to the data acquisition device (DAQ) for sampling and completed the measurement process of partial discharge signal in the connector. The measurement system is shown in Fig.11 (b).

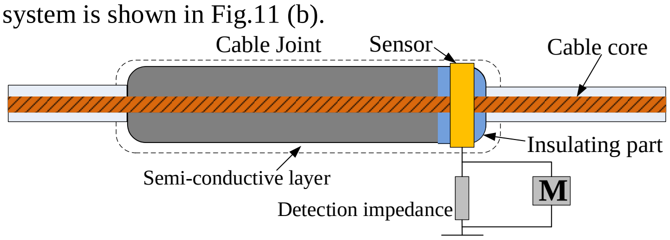

(a) Schematic diagram of the measurement system

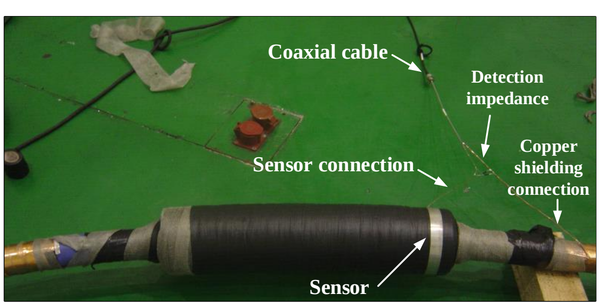

(b) Physical view of the measurement system

Figure 11 Structure diagram of partial discharge measurement system

With the developed capacitive sensor, the shielding effect of the semi-conductive layer outside the monolithic insulated joint is avoided and high sensitivity can be obtained. Moreover, the strip sensor is easy to be installed and the connection of wire is simple. The strip sensor is integrated with the joint without changing the structure of the cable joint so that the online detection of the partial discharge can be achieved.

We carried out 10 times of measurement under the standard PD pulse calibrator (Type: CAL 542, manufactured by OMICRON electronics Corp. USA) at 10 pC, 50 pC and 100 pC, respectively. The standard deviation of the repeatedly measured magnitude data is evaluated to quantitate the scatter of data around the calibrated PD values. The uncertainty value of the reported capacitive strip sensor is calculated as 2 pC.

Considered the characteristics of thermal expansion and contraction during long term operation, a buffer layer is filled between the insulating joints and strip sensor. The buffer layer was made of polyester film (PET), whose dielectric constant is very close to the material of silicon rubber insulation. The thickness of the buffer layer is 25 μm. The PET is installed tightly between the strip sensor and the outer surface of the joint.

B. Experimental setup of comparative PD detection

To establish the relationship between the measured output signal (mV) and the apparent discharge magnitude (pC), an experimental platform was set up. The test system of 110kV monolithic insulated joint is shown in Fig. 12. The two sections of 110 kV XLPE cable were connected by a monolithic insulated joint. Moreover, the cable terminal was connected to the water terminal to prevent the corona during the increased stressing high voltage. Besides, the cable core was connected to the testing transformer through the water terminal, and the outer shield of the cable is well grounded. The partial discharge measurement system proposed was connected to the test circuit, with the strip sensor wrapped around the insulating part of the monolithic insulated joint.

In Fig. 12, C was the coupling capacitance, and Z_m was the measuring impedance of the DST-4 standard partial discharge detector, according to IEC 60270 method.

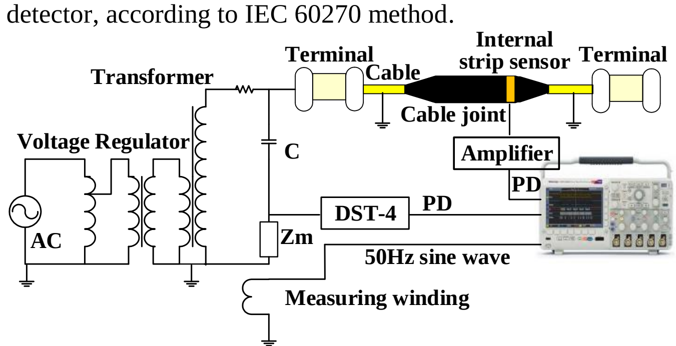

Figure 12 Partial discharge detection on the platform of 110 kV XLPE cable joints

In our experiments, PD tests were carried out according to IEC 60270 standard, results an uncertainty value given by the maximum of ±10% of the measurement or ±1 pC, whichever is the greater [30, 31]. DST-4, as a typically conventional partial discharge detector, performs charge determination of PD pulses with low uncertainty in accordance with IEC 60270. The oscilloscope was used to detect the strip sensor signal, DST-4 PD signal and the power frequency signal was from the measuring winding simultaneously. During this process, the power frequency signal was used as the trigger to obtain the phase information of the partial discharge information.

With regard to the compatibility, PD signal of the whole system was detected by standard PD detector before and after the introduction of the strip sensor. Under the voltage level of 160 kV, the PD signal was still lower than 5 pC, similar to the background signal level. That is to say, the installation of the strip sensor did not have a negative effect on the insulation properties of the monolithic insulated joint and the compatibility of two measurement system were guaranteed.

During the PD detection, the PD signal was measured by the strip sensor and standard detector synchronously. In our case, the detection band was set to 40 kHz-80 kHz. The detection sensitivity was not lower than 5 pC. To ensure the safety of the measurement equipment during the test, a parallel test loop was used during the experiment. The waveform of the developed strip sensor at apparent discharge quantities of 10 pC was shown in Fig. 13. The signal to noise ratio S/N is larger than 2, which means that the detection sensitivity of the developed partial discharge measurement system was also less than 5 pC.

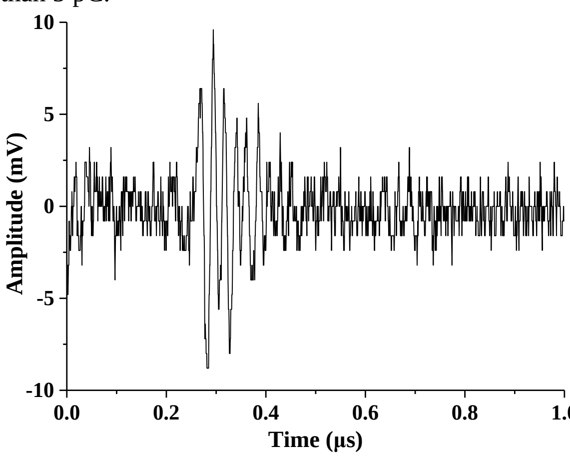

Figure 13 Waveform of the sensor at apparent discharge quantities of 10 pC

In the capacitive strip sensor system, the bandwidth of the amplifier filter was set to 50 MHz ~ 300 MHz, and the gain was set to 40 dB. In order to reduce the hardware requirements for high-frequency signals on the sampling rate of the back-end acquisition device, an amplifier with the function of peak value detection is used. After the demodulation process, the signal was sent to the back end acquisition device.

C. Analysis of experiment results

A copper pin of 2 mm diameter was inserted from the stress cone in the joint with a depth of about 8 cm. As a floating tip, the copper pin was designed as a suspended discharge failure between the XLPE insulation and the stress cone.

In order to further verify the consistency of the different PD measurement systems, the phase statistical characteristics of PD signals were analyzed and compared. Generally, it's available to describe the discharge repetition rate and the phase distribution of total discharge through φ-*n* and φ-q two-dimensional spectrum. *n* is the discharge repetition rate representing the average number of pulses per second during the discharge. q is apparent discharge magnitude. In this way, the influence of different number of detection cycles with regard to statistical discharge is avoided. The processing of the two-dimensional spectrum is as follows: dividing the frequency phase in the range of 360 degrees into 128 cells equally, and then the discharge repetition rate and total discharge in each cell are calculated. In order to analyze the characteristics of the discharge repetition rate and the distribution of the discharge in the phase systematically, the partial discharge gray scale was also analyzed. Firstly, the amplitude of the discharge was normalized with the φ-q norm plane. Then, the φ-q norm plane was divided into 128*128 minor cell. Besides, the discharge repetition rate in each cell was calculated in turn, and the mapping relationship between the discharge repetition rate and the color of the gray image was defined. Afterwards, the grayscale image of partial discharge was built according to the principle that the minimum/maximum values of the repetition rate in the cell were corresponded to the minimum/maximum gray level, respectively. The extreme normalized gray scale was obtained from the normalization of all the amplitudes of discharge according to the extreme value of the discharge in the test duration. In this way, the detailed characteristics of partial discharge in the stage could be better characterized. At last, the spectrums generated by the results of the two methods are shown in Fig.14 (a)-(c).

Fig.14 clearly shows that the phase distribution of the partial discharge signal detected by the two methods is nearly the same. In details, the discharge of the positive half-cycle was mainly distributed at 20 ~120 degrees, and the negative half-cycle mainly distributed at 190 ~270 degrees, only slightly different in the amplitude of the longitudinal axis. The repetition rates of the partial discharge signals were almost the same in the positive half-cycle. Moreover, in the negative half-cycle, the repetition rates of PD signal measured by the proposed strip sensor were a little lower than that of the standard PD detector with a consistently matched trend. With regard to φ-q total spectrum and normalized grayscale, the overall trends of PD signals detected by the two techniques were consistent with each other as well. The well matched results shown in Fig. 14 indicates the effectiveness of our designed strip sensor.

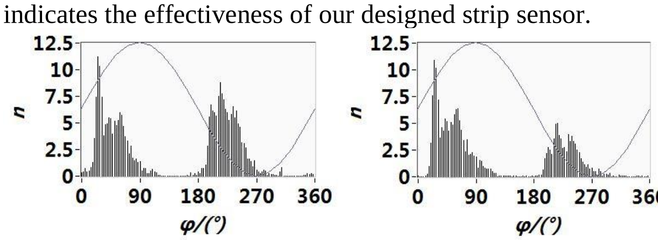

(a) φ-n Spectrum

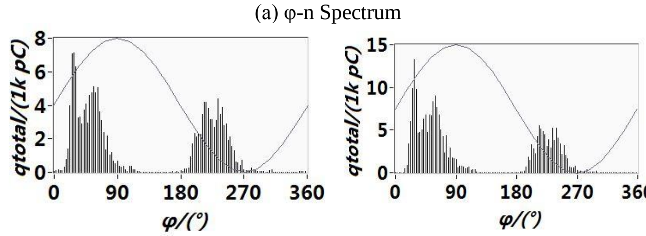

(b) φ-q total Spectrum

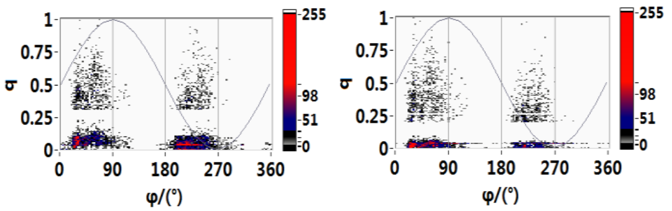

(c) Extreme value grayscale

Figure 14 PD spectrum of designed strip sensor (right) versus standard PD detector (left)

IV. Conclusion

To monitor the health status of power cable joints by partial discharge, a high-sensitivity, inside-the-joint, and easy-installation, capacitive strip sensor for high voltage XLPE cable joint is designed and tested in this study. A 3-dimensional model was built based on the finite integration technique at first to investigate the propagation law of partial discharge. It reveals that the electromagnetic wave is transmitted in the quasi-TEM mode, and the electric field intensity is the largest in the radial direction with the angle of 0° between PD source. The frequency spectrum of the PD signal concentrates in the range of 50 MHz - 300 MHz. Based on the results of FIT study, the best installation position for the PD detection sensor is identified. With those design insights, a real capacitive PD strip sensor is developed and comparative partial discharge tests with a standard PD detector have been conducted on a 110 kV cable joint platform. Consistent measurements with the standard PD detector have been observed and a high sensitivity of less than 5 pC, has been achieved. The tests clearly indicate the potential of our proposed capacitive strip sensor on the applications of online PD monitoring for high voltage power system cables.

References

[1]W. J. K. Raymond, H. A. Illias, and A. H. A. Bakar, "High noise tolerance feature extraction for partial discharge classification in XLPE cable joints," *IEEE T. Dielect. El. In.*, vol. 24, no. 1, pp. 66-74, 2017.

[2]C. Zhang, C. Li, L. Nie, Z. Jing, and B. Han, "Research on the water blade electrode method for assessing water tree resistance of cross-linked polyethylene," *Polym. Test*, vol. 50, pp. 235-240, 2016.

[3]K. Zhu, W. Han, W. K. Lee, and P. W. T. Pong, "On-Site Non-Invasive Current Monitoring of Multi-Core Underground Power Cables With a Magnetic-Field Sensing Platform at a Substation," *IEEE Sens J.*, vol. 17, no. 6, pp. 1837-1848, 2017.

[4]Y. Tian, P. L. Lewin, and A. E. Davies, "Comparison of on-line partial discharge detection methods for HV cable joints," *IEEE T. Dielect. El. In.*, vol. 9, no. 4, pp. 604-615, 2002.

[5]H. Orton, "Power cable technology review," *High Voltage Engineering*, vol. 41, pp. 1057-1067, 2015.

[6]V. Englund, R. Huuva, S. M. Gubanski, and T. Hjertberg, "High efficiency voltage stabilizers for XLPE cable insulation," *Polym Degrad Stabil.*, vol. 94, no. 5, pp. 823-833, 2009.

[7]F. Puletti, M. Olivieri, A. Cavallini, and G. Montanari, "Risk management of HV polymeric cables based on partial discharge assessment," in Proc. IEEE PES Transmission Distribution Conf, Dallas, TX, 2006, pp. 626-633.

[8]D. F. J. Jabha, K. Selvi, and R. Joselin, "A new approach for the failure prediction in XLPE power cables using acoustic emission technique," *Int J. Elec. Power*, vol. 81, pp. 336-345, 2016.

[9]T. Zhang, F. Pang, H. Liu, J. Cheng, L. Lv, X. Zhang, et al., "A Fiber-Optic Sensor for Acoustic Emission Detection in a High Voltage Cable System," *Sensors-Basel*, vol. 16, no. 12, 2016.

[10] P. Lewin, L. Hao, D. Swaffield, and S. Swingler, "Condition monitoring of power cables," *IET Power Convention*, pp. 1-7, 2007.

[11] Y. Tian, P. Lewin, J. Wilkinson, G. Schroeder, S. Sutton, and S. Swingler, "An improved optically based PD detection system for continuous on-line monitoring of HV cables," *IEEE T. Dielect. El. In.*, vol. 12, no. 6, pp. 1222-1234, 2005.

[12] C. Volat, M. Jabbari, M. Farzaneh, and L. Duvillaret, "New method for in live-line detection of small defects in composite insulator based on electro-optic E-field sensor," *IEEE T. Dielect. El. In.*, vol. 20, no. 1, pp. 194-201, 2013.

[13] M. Wu, H. Cao, J. Cao, H. L. Nguyen, J. B. Gomes, and S. P. Krishnaswamy, "An overview of state-of-the-art partial discharge analysis techniques for condition monitoring," *IEEE Electr. Insul. M.*, vol. 31, no. 6, pp. 22-35, 2015.

[14] A. Rodrigo Mor, L. C. Castro Heredia, D. A. Harmsen, and F. A. Muñoz, "A new design of a test platform for testing multiple partial discharge sources," *Int J. Elec. Power*, vol. 94, pp. 374-384, 2018.

[15] M. N. K. H. Rohani, C. C. Yii, M. Isa, S. I. S. Hassan, B. Ismail, M. R. Adzman, et al., "Geometrical Shapes Impact on the Performance of ABS-Based Coreless Inductive Sensors for PD Measurement in HV Power Cables," *IEEE Sens J.*, vol. 16, no. 17, pp. 6625-6632, 2016.

[16] N. Marukatat, A. Kunakorn, P. Yutthagowith, and S. Pumyoy, "Design and analysis of coupling device in partial discharge detection," in Proc. 2017 International Symposium on Electrical Insulating Materials (ISEIM), Toyohashi, Japan, 2017, pp. 386-389.

[17] X. Gu, Y. Xu, R. Xia, S. Meng, and Y. Wang, "On-line calibration of partial discharge monitoring for power cable by HFCT method," in Proc. IEEE Electrical Insulation Conference (EIC), Montreal, Canada, pp. 40-44, 2016.

[18] Y. Xu, X. Gu, B. Liu, B. Hui, Z. Ren, and S. Meng, "Special requirements of high frequency current transformers in the on-line detection of partial discharges in power cables," *IEEE Electr. Insul. M.*, vol. 32, no. 6, pp. 8-19, 2016.

[19] G. Dai, S. Jing, and Z. Ziyu, "Research on directional coupler measurement in partial discharge monitoring of XLPE cable," in Proc. 2014 International Symposium on Electrical Insulating Materials, Niigata, JAPAN, 2014, pp. 253-256.

[20] W. He, H. Li, D. Liang, H. Sun, Z. Sun, and B. Liu, "An Improved Directional Sensor for On-line Partial Discharge Measurement in Overhead Covered Conductors," *Electr. Pow. Compo. Sys.*, vol. 44, no. 14, pp. 1543-1550, 2016.

[21] N. Ra, N. S. B. Mustafa, H. Futami, T. Kawashima, Y. Murakami, N. Hozumi, et al., "Development of the new partial discharge measuring method and device for long power cable using foil electrode," in Proc. 2017 International Symposium on Electrical Insulating Materials (ISEIM), Toyohashi, Japan, 2017, pp. 347-350.

[22] F. Álvarez, F. Garnacho, J. Ortego, and M. Á. Sánchez-Urán, "Application of HFCT and UHF sensors in on-line partial discharge measurements for insulation diagnosis of high voltage equipment," *Sensors-Basel*, vol. 15, no. 4, pp. 7360-7387, 2015.

[23] R. Sarathi and R. Umamaheswari, "Understanding the partial discharge activity generated due to particle movement in a composite insulation under AC voltages," *INT J. Elec. Power*, vol. 48, pp. 1-9, 2013.

[24] L. Zhong, G. Chen, and Y. Xu, "A novel calibration method for PD measurements in power cables and joints using capacitive couplers," *MEAS SCI Technol.*, vol. 15, no. 2, pp. 1892-1896, 2004.

[25] V. Dubickas, "On-line time domain reflectometry diagnostics of medium voltage XLPE power cables," KTH, 2006.

[26] W. Choi, J. T. Kim, I. J. Seo, J. S. Hwang, and J.-Y. Koo, "Development of a partial discharge detection algorithm and verification test for extra-high-voltage cable system," *IET Science, Measurement & Technology*, vol. 10, no. 2, pp. 111-119, 2016.

[27] Z. H. Shao and N. Bowler, "Capacitive Nondestructive Evaluation of Aged Cross-Linked Polyethylene (XLPE) Cable Insulation Material," in Proc. 18th International Conference on Environmental Degradation of Materials in Nuclear Power Systems Water Reactors, J. H. Jackson, D. Paraventi, Springer International Publishing, 2018, pp. 87-97.

[28] Heinrich R., S. Bonisch, D. Pommerenke, R. Jobava, and W. Kalkner. "Broadband measurement of the conductivity and the permittivity of semiconducting materials in high voltage XLPE cables." in Proc. 8th International Conference on Dielectric Materials, Measurements and Applications, Edinburgh, Scotland, 2000, pp. 212-217.

[29] Ma G. M., Li C. R., Chen X. W., Jiang J., Ge Z. D. and Chang, W. Z., "Numerical sensor design for partial discharge detection on power cable joint," *IEEE T. Dielect. El. In.*, vol. 22, no. 4, pp. 2311-2319, 2015.

[30] IEC 60270, "High-voltage test techniques – Partial discharge measurements," 2015

[31] L. W. van Veen, "Comparison of measurement methods for partial discharge measurement in power cables", Delft university of technology, 2014.